

## Supporting Information

# Delivery of Cargo with a Bioelectronic Trigger

*Zahra Hemmatian<sup>†, 1</sup>, Elmira Jalilian <sup>§, ⊥, #, 1</sup>, Sangeun Lee <sup>Δ</sup>, Xenofon Strakosas <sup>†</sup>, Ali Khademhosseini <sup>§, ⊥, π, \$, &, ω, +, ¶</sup>, Adah Almutairi <sup>Δ, ψ \*</sup>, Su Ryon Shin <sup>§, ⊥\*</sup>, Marco Rolandi <sup>†\*</sup>*

<sup>†</sup> Department of Electrical Engineering, University of California Santa Cruz, Santa Cruz, California 95064, USA.

<sup>§</sup> Division of Engineering in Medicine and Department of Medicine, Brigham and Women's Hospital, Harvard Medical School, Boston, MA 02139, USA.

<sup>⊥</sup> Harvard-MIT Division of Health Sciences and Technology, Massachusetts Institute of Technology, Cambridge, MA 02139, USA.

<sup>#</sup> UCL Institute of Ophthalmology, University College London, London, United Kingdom.

<sup>Δ</sup> UCSD Center of Excellence, Department of NanoEngineering, Jacobs School of Engineering, University of California San Diego, 9500 Gilman Dr., La Jolla, California 92093, USA.

<sup>π</sup> Center for Nanotechnology and Department of Physics, King Abdulaziz University, Jeddah 21569, Saudi Arabia.

<sup>§</sup> Department of Bioindustrial Technologies, College of Animal Bioscience and Technology, Konkuk University, Seoul 143-701, Republic of Korea.

<sup>&</sup> Department of Bioengineering, Department of Chemical and Biomolecular Engineering, Henry Samueli School of Engineering and Applied Sciences, University of California-Los Angeles, Los Angeles, CA, USA.

<sup>ω</sup> Department of Radiology, David Geffen School of Medicine, University of California-Los Angeles, Los Angeles, CA, USA.

<sup>+</sup> Center for Minimally Invasive Therapeutics (C-MIT), University of California-Los Angeles, Los Angeles, CA, USA.

<sup>¶</sup> California NanoSystems Institute (CNSI), University of California-Los Angeles, Los Angeles, CA, USA.

<sup>ψ</sup> Skaggs School of Pharmacy and Pharmaceutical Sciences, University of California at San Diego, 9500 Gilman Dr., La Jolla, California 92093, USA.

<sup>1</sup> These authors have equal contribution.

\*Email: [mrolandi@ucsc.edu](mailto:mrolandi@ucsc.edu) (M. R.)

\*Email: [aalmutairi@ucsd.edu](mailto:aalmutairi@ucsd.edu) (A. A.)

\*Email: [sshin4@bwh.harvard.edu](mailto:sshin4@bwh.harvard.edu) (S. R. S.)

## EXPERIMENTAL SECTION.

*Bioprotonic pH modulator:* The protonic devices are fabricated on microscope glass slide (2.5cm x 4.5cm VWR). 100 nm Pd with a 15 nm Cr adhesion layer in the area of 12 mm<sup>2</sup> is deposited via e-beam evaporation (Balzers PLS 500). The Pd surface is coated with a layer of Pd nanoparticles (PdNPs) via electrochemical deposition. Polydimethylsiloxane (PDMS) wells are used as solution containers and attached to the Pd substrates with PDMS. For the pH modulation in the physiological condition Ag/AgCl pellet electrodes are used as a Counter Electrode (CE), Ag/AgCl glass electrode is used as Reference Electrode (RE) and Pd/ Pd NPs contact are used as Working Electrode (WE). Electrochemical measurements are performed with a potentiostat from Metrohm.<sup>1</sup>

*Electrical measurements:* All electrical measurements were performed using Potentiostat PGSTAT128N with FRA32M Module from Metrohm.

*Microscope images:* The Fluorescence images of the MPs were collected using a BZ-series fluorescence microscopy of BZ-X710 from Keyence.

*Scanning Electron Microscopy (SEM):* SEM measurements were performed by a Quanta 3D FEG of Secondary electron detection (standard SEM) in Dual-Beam Microscope User Facility at UCSC. Before doing the SEM measurements, the samples were coated with 5nm of Au. By using a precise view of the surface of Pd contact following the Au deposition, based on the optimal duration for the electrodeposition of PdNPs we could determine the number and spacing of individual PdNPs. We also determined the shape of the MPs before and after degradation using SEM characterization.

*Fluorescence measurements:* All the fluorescence intensity (FI) measurements were performed by a fluorometer from Horiba scientific Model FluoroMax-3.

*Synthesis of pH-sensitive AcDex Microparticles (MPs):* pH-sensitive acetalated dextran (Ac-Dex) was synthesized by following and modifying a previously described method. Dextran (10 – 12 kDa, from *Leuconostoc mesenteroides*), 3 g (18.5 mmol), was dissolved in 27 ml of anhydrous dimethyl sulfoxide (DMSO) and followed by addition of *p*-toluenesulfonic acid (18 mg, 71.6 mmol). After 15 min, 2-methoxypropene (10.2 ml, 106.37 mmol) was slowly added into the solution and stirred at room temperature. After 3 hrs, the reaction was quenched with 5 mL triethylamine. The newly synthesized polymer was precipitated in 0.01% trimethylamine containing water. This precipitation process was repeated three times to further purify the polymer. The product was a white solid (3.34 g, 84 % yield). Rhodamine conjugated Ac-Dex was also prepared for particle tracking. It was synthesized with same method by acetalizing rhodamine conjugated dextran (10 kDa). pH sensitivity is affected by the ratio of cyclic to acyclic acetal groups. To calculate cyclic ratio of the resulting Ac-Dex, the suspension of Ac-Dex in D<sub>2</sub>O was added a small amount of deuterium chloride (1 % DCl). The cyclic ratio was calculated by comparing proton NMR peaks of acetone and methanol.<sup>2</sup> As a result, cyclic ratio of acetalated polymer (Ac-Dex) was 66 %.

*Microparticle formulation:* Ac-Dex, 60 mg, and 6 mg of Lutrol F 126 were dissolved in 80  $\mu$ l of DMSO and 320  $\mu$ l of CHCl<sub>3</sub>. The polymer solution was injected into a capillary tube with a flow rate of 0.18 ml/min. A voltage of ~ 16 kV was applied and the particles were collected onto slides. Sprayed particles were dried for overnight in a desiccator.



Dried particles were re-dissolved in PBS and washed 3 times by centrifuge (4500 rpm, 10 min, 20 °C).

*pH-triggered MPs deformation:* 0.1 mg/mL Ac-Dex MPs in pH= 6.0 and pH= 7.4 phosphate buffer were incubated at 37 °C for 2 days. The incubated MPs are diluted with H<sub>2</sub>O and put on a silicon wafer. After drying overnight under vacuum, the MPs are coated by a sputter coater and observed by SEM.

*pH-triggered cargo release from MPs:* 1 mg of FDA loaded Ac-Dex MPs were dissolved in 10 mL of pH 6.0 and pH 7.4 phosphate buffer. The MPs solutions are incubated at 37 °C and released FDA was separated from MPs by centrifugation (13000 rpm, 10 min, 20 °C) at each time point. The collected FDA was hydrolyzed by 1 M NaOH and emission was measured by fluorometer (Figure SI 5).

*Fibroblast cell culture:* In order to verify the delivery of pH-sensitive FDA-loaded Rho-AC-Dex particles into the cells and evaluate the release of FDA into the cells, cardiac fibroblasts (CFs) were isolated from 1 to 2 day old neonatal Sprague Dawley rats using a protocol approved by the Institute's Committee on Animal Care<sup>3</sup> and were used as cells of interest.<sup>4</sup> Cells were cultivated in DMEM-high glucose medium (Gibco-11965-092) supplemented with 10 % FBS (Gibco, 10437-028), 1 % L- Glutamine (Gibco, 25030-081), 1 % penicillin/streptomycin. Cardiac fibroblasts were used between passages 2-5. Each Pd NP protonic device were washed with several times with 70 % ethanol and coated with 10 % fibronectin for 1hr in room temperature. Cells were seeded at the density of  $1.6 \times 10^5$  cells/cm<sup>2</sup> and left for 48 hrs to settle. Then, Rho-AC-Dex particles were added in the same medium and at the concentration of 0.5 mg/ml. Then MPs were

sonicated in a water sonicator bath for 5 min and then were centrifuged at 3000 rpm for 15 min at 20 °C. Supernatant were removed and MPs re-suspended in medium and washing step repeated one more time. Then cardiac fibroblasts were incubated with MPs dispersed medium for 1 hr. To make pH 6.0 culture condition for particles to release FDA, appropriate amount of 0.1M HCL were added to the medium containing MPs (previously optimized) soon after adding the MPs to the cells. In the case of bioelectronic pH stimulation, media solution containing MPs in neutral pH (7.4) was added to the cells seeded on Pd/ Pd NPs contact and the flow of  $H^+$  from the contact to the solution provides upon application of  $V = 0.3 \text{ V}$  vs. Ag/AgCl for 40 sec. After 1 hr cells were washed with medium for few minutes to and cells were assessed for FDA-release using fluorescent microscopy.

*Microscope images:* All microscope images were performed using fluorescence microscope (Axio Observer D1, Carl Zeiss) and Image J software was used for analysis.

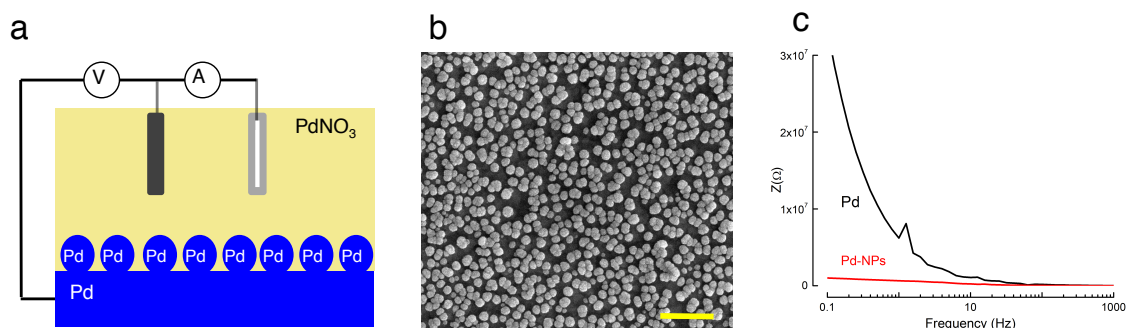


**Figure SI 1.** (a) The scheme of electrochemical deposition of Pd NPs to improve  $H^+$  transport in buffer condition. Planar Pd is used as working electrode (WE), Ag/AgCl as a reference electrode (RE) and Pd wire as a counter electrode (CE). We added 100 mg/ml PdNO<sub>3</sub> solution into the PDMS well and we applied a potential difference of  $V = -0.8V$  between Pd and RE for 100 sec to deposit Pd NPs. (b) SEM images of the Pd NPs deposited on the planar Pd contact. The scale bar is 500nm. The NPs has the size of ca. 70 nm ( $\pm 5$ ). (c) Electrochemical impedance spectroscopy (Bode plot) shows the impedance of a planar Pd contact (black trace) and planar Pd contact coated with Pd NPs in a PBS 1x pH= 7.4. Pd contact is used as a WE and Ag/AgCl electrodes is used as a RE and CE. The impedance as a function of frequency plot was recorded when a 10mV AC signal was applied at frequencies ranging from 0.1Hz to 100kHz. It shows that the Pd planar contact coated with Pd NPs exhibits lower impedance than planar Pd contact. It is inversely proportional to the higher capacitance of the Pd contact coated with Pd NPs compare to planar Pd contact.

To calculate the surface area of the Pd contact coated with Pd NPs we first calculate the surface area of single NPs according to the size of the NPs ca. 70nm ( $\pm 5$ ) measured by SEM, Area of Circle ( $A_C$ )  $A_C = \Pi r^2$ , where  $\Pi = 3.14$  and  $r$  is the radius. Considering the surface area of the planar Pd contact ca. 12 mm<sup>2</sup> and the surface area of a single Pd NPs ca.  $3.85 \times 10^{-9}$  mm<sup>2</sup> we estimate the number of Pd NPs coated the surface  $\sim 3 \times 10^9$ . Because the NPs have the spherical shape we then calculate the surface area of Pd NPs ca. 46 mm<sup>2</sup>, with Area of Spherical ( $A_S$ ),  $A_S = 4 \Pi r^2$ , and considering the estimated number of Pd NPs. Since the spacing between Pd NPs collected by SEM images is the same as the size of Pd NPs, therefore the final surface area of the Pd contact coated with Pd NPs is 52 mm<sup>2</sup>. Comparing the surface area of the planar Pd ca. 12 mm<sup>2</sup> the surface area of the Pd contact coated with Pd NPs is  $\sim 4$  times higher than planar Pd contact.

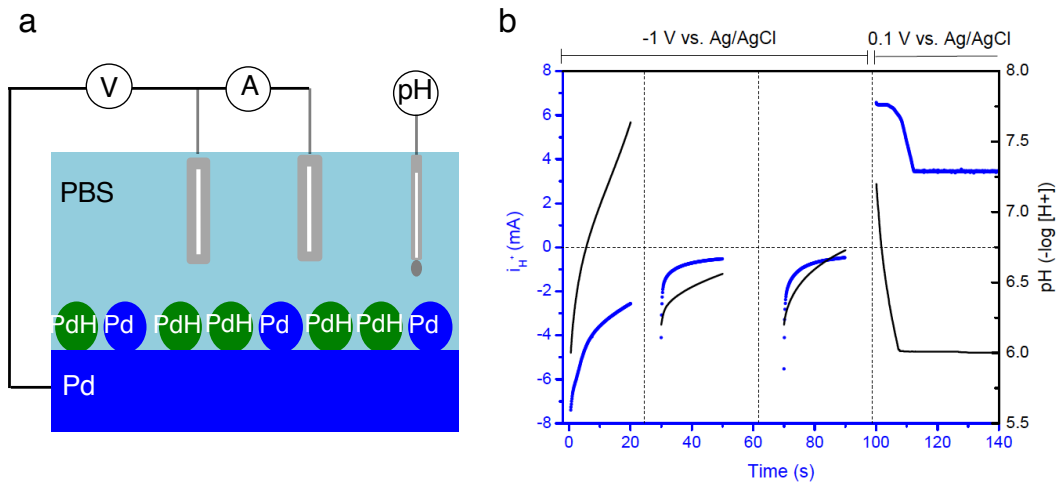


**Figure SI 2.** (a) The scheme of the Pd contact device coated with Pd NPs that provides the transport of H<sup>+</sup> from/ to Pd NPs contact upon application of voltage (V). (b) The proton current ( $i_{H^+}$ ) vs time graph (blue trace) and the calculated pH vs time graph (black

trace). The PDMS well was filled with 100ml PBS 1x, pH=6.0. We applied  $V = -1.0$  V vs. RE for 20sec. The proton current changed from  $i_{H^+} = -7.40 \times 10^{-3}$  A to  $i_{H^+} = -2.56 \times 10^{-3}$  A (black trace). From the total charge collected to the leads we calculated the pH changes (Note SI 1) for the first 20 sec. The pH changed from pH= 6.0 to pH= 7.8 (black trace). We then replaced the solution with a fresh PBS 1x, pH= 6.0 and we applied  $V = -1.0$  V vs RE for the second 20 sec. The proton current changed from  $i_{H^+} = -4.11 \times 10^{-3}$  A to  $i_{H^+} = -0.53 \times 10^{-3}$  A (blue trace). Which correspond to the change of pH from pH= 6.2 to pH= 6.55 (black trace). We again replaced the solution with fresh PBS 1x, pH= 6.0 and we applied  $V = -1.0$  V vs RE for the third 20 sec. The proton current changed from  $i_{H^+} = -5.53 \times 10^{-3}$  A to  $i_{H^+} = -0.47 \times 10^{-3}$  A (blue trace). Which correspond to the change of pH from pH= 6.2 to pH= 6.7 (black trace). To transport the  $H^+$  to the solution and bring it to acidic condition, we then replaced the solution with the fresh PBS 1x, pH= 7.4 and we applied  $V = +0.1$  V vs RE for 40sec. The proton current changed from  $i_{H^+} = +6.75 \times 10^{-3}$  A to  $i_{H^+} = +3.47 \times 10^{-3}$  A (blue trace). Which correspond to the change of pH from pH= 7.2 to pH= 6.0 (black trace).

## Note SI 1

The area under the  $i_{H^+}$  vs. time graph results the charge transport of  $H^+$ . We calculate the concentration of  $H^+$ ,  $[H^+]$ , in 100  $\mu$ l of buffer solution using Faraday constant, 96485.33289 C mol<sup>-1</sup>. We then calculate the pH change in PBS buffer solution using the "*Henderson Hasselbalch Equation*"<sup>5</sup>.

$$pH = pK_2 + \log \frac{[HPO_4^{2-}]}{[H_2PO_4^-]} \quad (1)$$

$$K_2 = \frac{[H^+][HPO_4^{2-}]}{[H_2PO_4^-]} ; [H^+] = \frac{K_2[H_2PO_4^-]}{[HPO_4^{2-}]} \quad (1)$$

,which can be converted to:

$$pH = pK_2 + \log \frac{[HPO_4^{2-}]}{[H_2PO_4^-]} \quad (2)$$

where  $pH = -\log[H^+]$ , and  $pK_2 = -\log K_2$ . The latter logarithmic expression called the "*Henderson Hasselbalch Equation*" is a convenient form to use in buffer calculations, particularly when the pH is within one unit above or one unit below the pK. (Where the ratio  $[HPO_4^{2-}]/[H_2PO_4^-]$  is between 0.10 and 10). Although all four species of phosphate are always present in solution, the two forms in the equation are the predominant ones near the pK and the others can usually be ignored in calculations. As one gets more than two units above or below the pK, however, other species become involved and the calculations get more complicated.

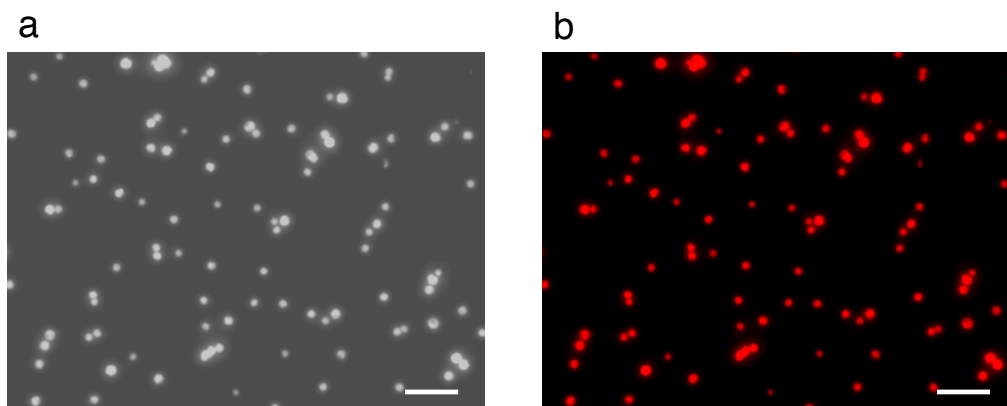


**Figure SI 3.** Microscopy image of MPs incubated in PBS 1x, pH= 7.4 (a) the dark field image and (b) the rhodamine fluorescence channel image evaluate that the size of MPs ca. is  $2.12 \pm 0.41 \mu\text{m}$ . The data are collected from 3 different Images. The red color is corresponding to conjugated rhodamine dye on the Ac-Dex polymer. The scale bare in the images is  $10 \mu\text{m}$ .

### Calculation of cyclic to acyclic ratio of Ac-Dex

The acetal ratio of cyclic to acyclic was calculated based on  $^1\text{H}$ -NMR. Ac-De polymer (5 mg) was dispersed in 1 ml of  $\text{D}_2\text{O}$ , and DCl was added on the solution. After 5 minutes of vortex, proton peaks were evaluated by NMR spectroscopy. Since cyclic acetals resulting acetone by hydrolysis while acyclic acetals resulting methanol and acetone, integration values of the methanol peak (3.34 ppm) and acetone peak (2.08 ppm) were compared to calculate cyclic to acyclic ratio, as previously described.<sup>2</sup> Consequently, 66 % of acetals were cyclic.

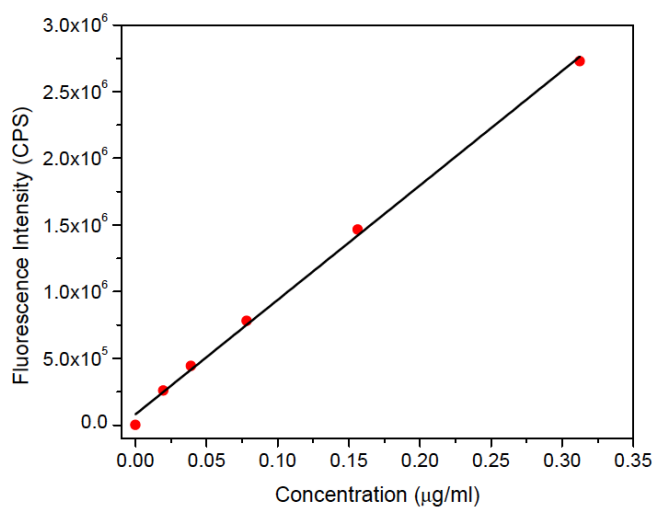


**Figure SI 4.** Fluorescein calibration curve for calculation of released FDA. We suspended the FDA into PBS 1x pH= 7.4 for the final concentration of 0 µg/ml, 0.02 µg/ml, 0.04 µg/ml, 0.08 µg/ml, 0.15 µg/ml and 0.30 µg/ml. For each of these samples we measured the Fluorescence intensity of the FDA solution upon addition of 1:1 0.2 mM NaOH to hydrolyze the FDA. We then plotted the Fluorescence intensity of known FDA solution vs. the corresponding concentration. We fit the experimental data with the linear fitting to obtain the calibration curve of  $Y = 4 \times 10^6 X + 34328$  ( $R^2 = 0.9981$ ). We then



used this calibration curve to calculate the released FDA from the MPs from the measured fluorescence intensity.

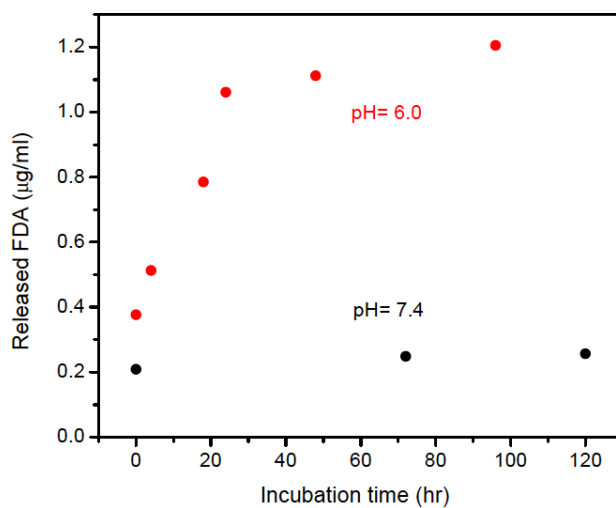


**Figure SI 5.** Release of FDA from Ac-Dex MPs at pH 6.0 (black) and pH 7.4 (red). We used the calibration curve (Figure SI 4) to convert the measured fluorescence intensity to the released FDA.

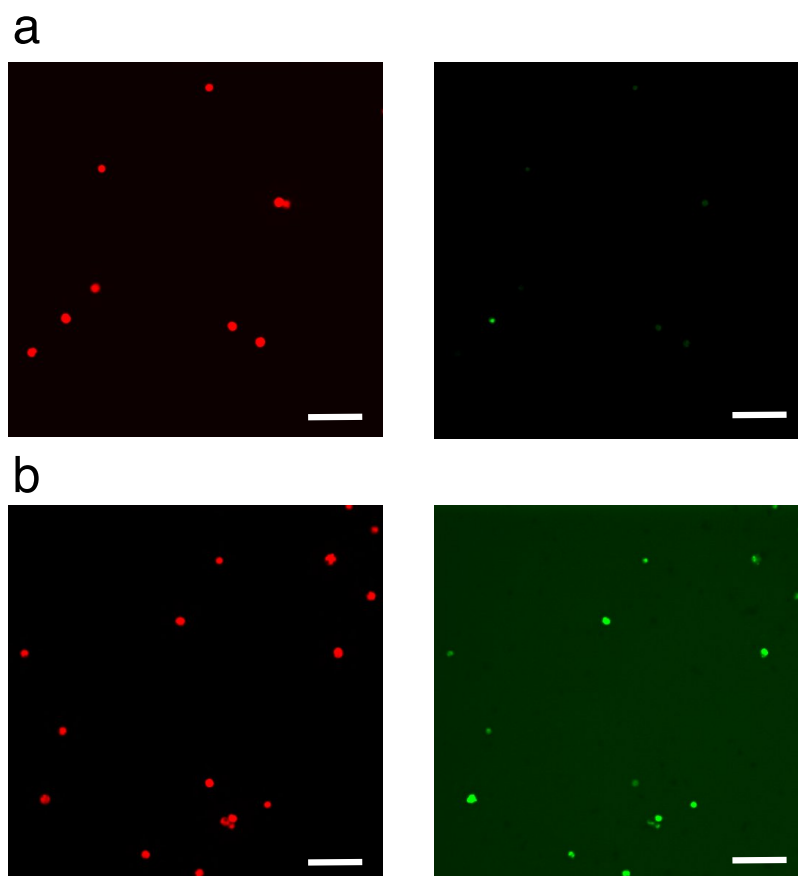


**Figure SI 6.** (a) The microscopy images of the MPs before bioelectronics trigger. The red color (left) is corresponding to the presence of rhodamine dye that is attached to the Ac-Dex MPs to be detectable. The size of MPs is  $\sim 2 \mu\text{m}$ . The green color and its corresponding fluorescence intensity (right) have very low intensity of ca. 0.07 RFU ( $\pm 0.02$ ), which confirms that FDA is still encapsulated inside the MPs. (b) The microscopy images of the MPs after bioelectronics trigger. The red channel image (left) is the MPs 2 hrs after bioelectronics trigger. No significant change observes for the size of MPs while they were in the solution. But the green color (right) and its fluorescence intensity has high intensity of ca. 2.4 RFU ( $\pm 0.3$ ) for MPs as well as the background solution, which confirms that FDA is released and hydrolyzed upon addition of 0.2 mM NaOH. The data

is collected from 3 different images for each condition. The images are analyzed under stack mode ROI method with equal intensity, brightness and contrast. The scale bar in images is 10  $\mu\text{m}$ .

### **Viability test in different concentrations of pH-sensitive MPs in 3T3 cells**

We investigated the optimum condition (MPs concentration and optimised pH) in which cells had the highest viability. We first investigated the pH-sensitive MPs (size: 2.12  $\mu\text{m}$  ( $\pm 0.41$ )) in three different concentrations (100, 500 and 1000  $\mu\text{g/ml}$ ). Prestoblue viability test illustrated significant reduction ( $*P < 0.05$ ) in cell viability in 1000  $\mu\text{g/ml}$  concentration compared to control condition. Furthermore, considerable reduction in cell density and several areas of particle aggregation was observed in 1000  $\mu\text{g/ml}$  concentration using phase-contrast microscopy. However, cells in concentrations of 100 and 500  $\mu\text{g/ml}$  showed similar viability and density compared to control condition. Therefore, 500  $\mu\text{g/ml}$  was chosen as the optimum concentration for pH-sensitive MPs (Figure SI 7 a, b). In the next step, in order to find out the toxicity of different pH on cell viability, cells were stimulated with 500  $\mu\text{g/ml}$  MPs in three different pH (5.0, 6.0 and 7.4) and compared to control condition. Control condition just contained medium in different pH condition. Prestoblue viability test showed significant reduction ( $*P < 0.05$ ) in cell viability in pH 5 compared to pH 6 and 7.4 in both control and stimulated cells with particles. Therefore, pH 5 considered to be toxic for the cells. Thus, pH 6 and 500  $\mu\text{g/ml}$  concentration was selected as the optimised condition (Figure SI 7 c, d).

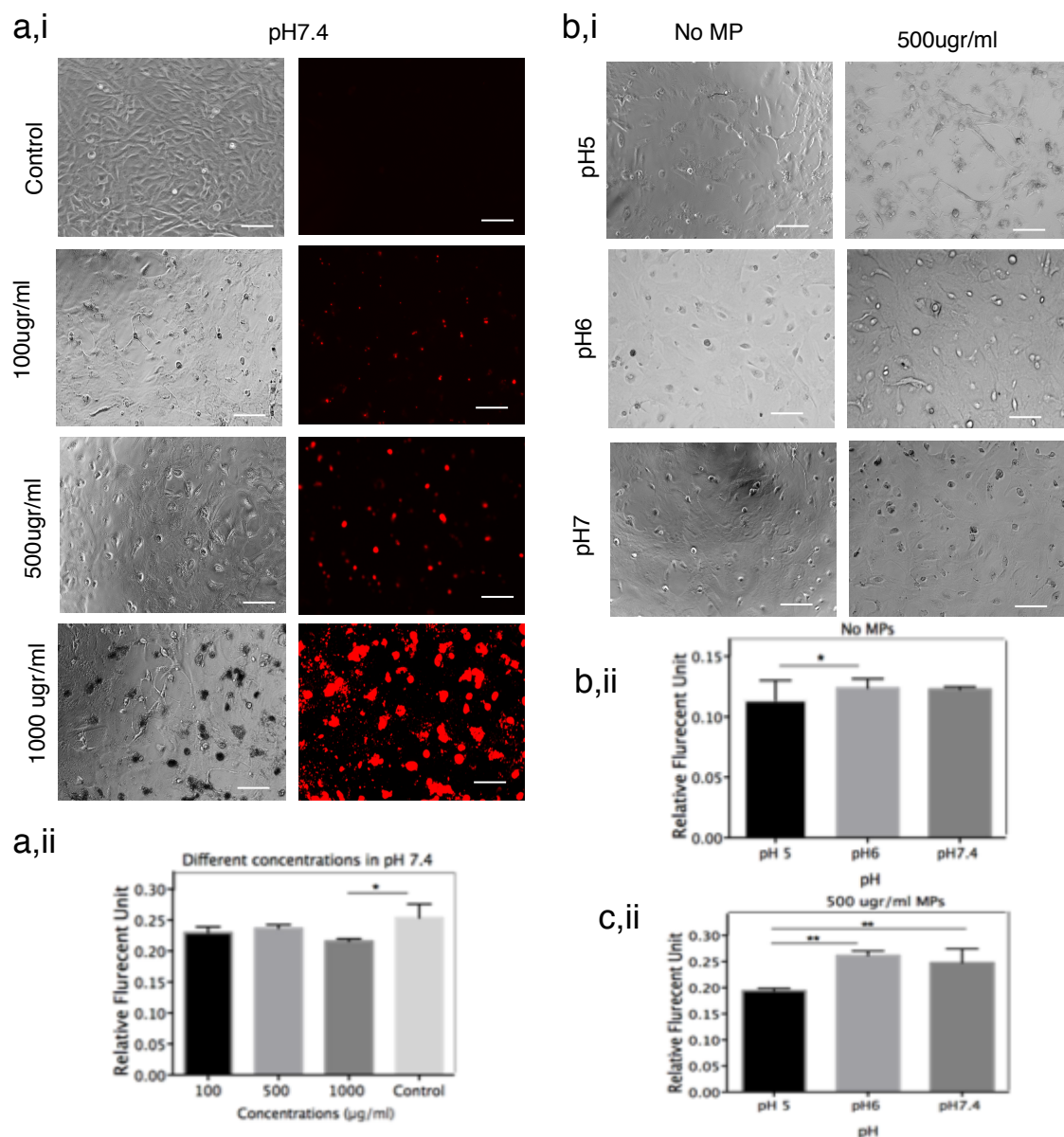


**Figure SI 7.** Optimization of the concentration and pH for MPs; (a) Representative images of cells in presence of MPs in different concentrations (100, 500 & 1000 µg/ml). Phase contrast microscopy were used to assess the cell morphology and density which showed big areas of cell death in 1000 µg/ml. Also, assessing Rhodamine-conjugated to particles in red channel showed increased aggregation pf particles in 1000 µg/ml. (b) Cell viability test in different concentrations of pH-sensitive MPs; Statistical

analysis (using prestoblue) showed significant reduction ( $*P < 0.05$ ) in 1000  $\mu\text{g/ml}$  concentration compared to other conditions. Scale bar 100 $\mu\text{m}$  (biological replicate=3 times & Technical replicate= 5 for each concentration). (c) Cells were cultured in three different pH 5, 6 7.4 (first row). Phase contrast microscope showed remarkable reduction in cell density and morphology. (d) Cell viability test showed significant reduction ( $*P < 0.05$ ) in cell viability. (e &f) Finally, cells were stimulated with optimum concentration of MPs 500  $\mu\text{g/ml}$  in three different pH. Phase contrast microscope showed remarkable reduction in cell density which was confirmed with cell viability test. Scale bar 100 $\mu\text{m}$ .

### Cell attachment and viability on bioelectronic trigger device

In order to find whether cells can attach to the Pd NPs surface, devices were first washed with 70% ethanol. Then they were washed 3 times with PBS + 5% Pen-Strep and then coated with fibronectin (10  $\mu\text{g/ml}$ ). Cells were then seeded in  $1.6 \times 10^5$  cells/ $\text{cm}^2$  in DMEM+10% FBS and left for 48 hrs to settle. Then, cells were fixed with 4% PFA and stained for F-actin and DAPI. Furthermore, cells were stained with LIVE/DEAD Cell Viability Assay to discriminate the population of live cells from dead-cell population and quantified using ImageJ. Percentage of dead cells (61 %) were approximately two times more than live cells (39 %). F-actin staining showed considerable amount of cell attachment to the surface.

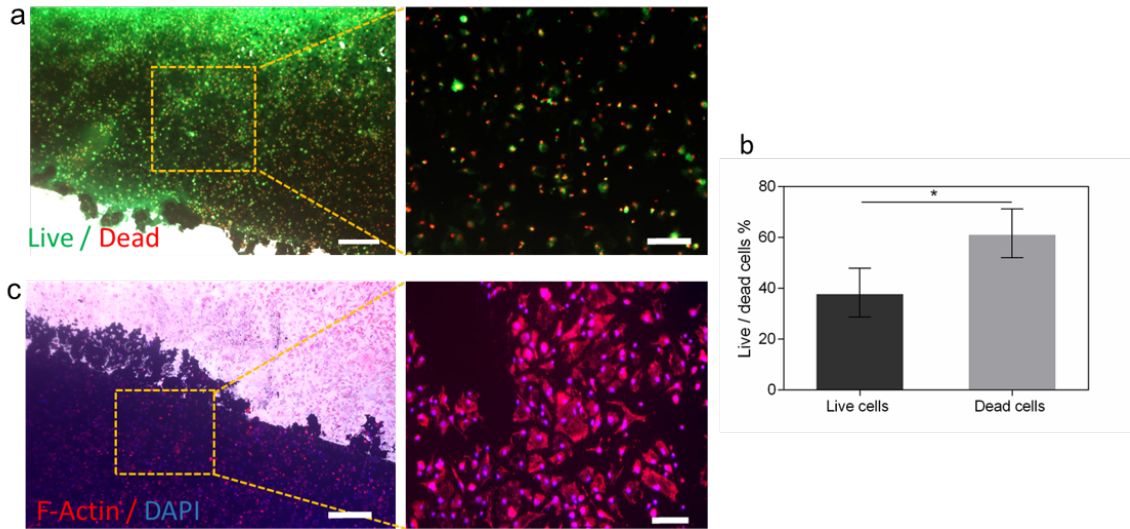


**Figure SI 8:** Assessment of cell attachment on Pd NPs surface. (a) LIVE/DEAD staining illustrates live cells in green and dead cells in red. (b) Quantification of live and dead cells showed significant difference ( $*P < 0.005$ ) between live and dead cells. (c) Cells were stained for F-actin and DAPI to better observe cell attachment to the surface. Scale bar for the two left images is 500 $\mu\text{m}$  and for the two right images are 200 $\mu\text{m}$ .

### Assessment of FDA uptake with manual stimulation

In order to assess the uptake of FDA with manual pH stimulation cardiac fibroblast cells were seeded on fibronectin coated PdNP protonic device and left for overnight to settle. After 24 hrs, medium containing MPs were added to the cells. Then appropriate amount of 0.1M HCl were added to the media to reach the pH 6. Uptaken of FDA were assessed under the microscope at time zero, 1 hr and 6 hrs respectively. Fluorescent microscopy observations illustrated that FDA was uptaken within the cells after 1 hr and 6 hrs at pH 6 whereas no FDA was uptaken within the cells even after 6 hrs at pH 7.4. Statistical analysis showed this difference was significant. (\*\* $P < 0.005$ ).

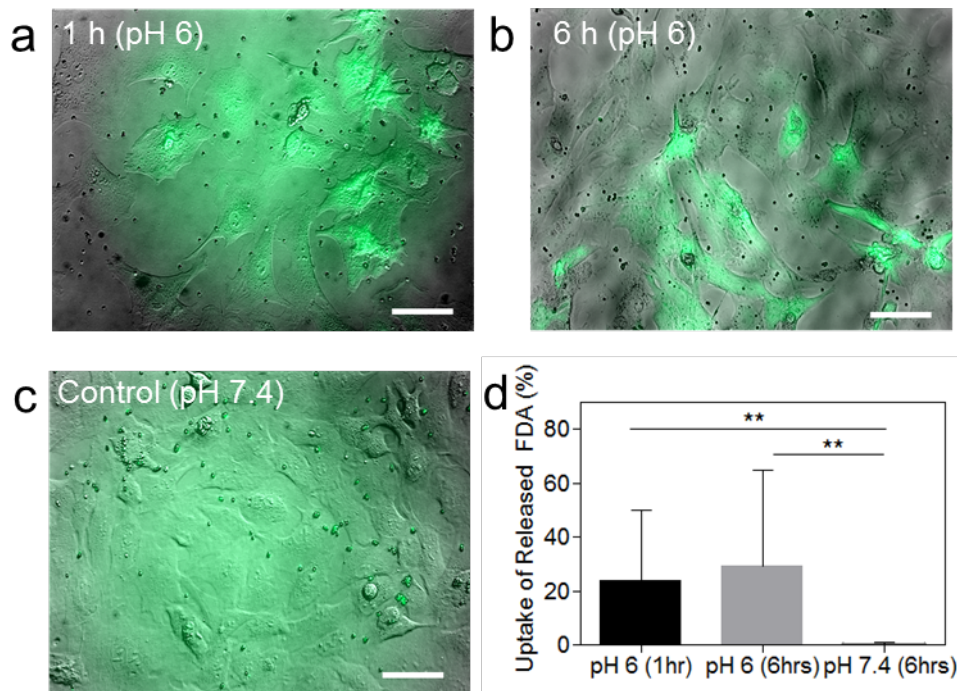


**Figure SI 9.** The uptake of FDA in different pH and time courses; Florescent microscopy observations showed that cells have uptaken the FDA 1hr after stimulation (a) which was also observed after 6hrs (b). No FDA up taken was observed in control condition (c).



Statistical analysis further confirms the significant difference between different FDA up taken in pH 6 (both 1hr and 6 hrs) versus pH 7.4 (d). Scale bar 50 $\mu$ m.

### Assessment of cell morphology at different pH values

In order to see the effect of acid treatment on cell morphology, cardiac fibroblast cells were seeded on 96 well-plates  $2 \times 10^4$  cells/well on DMEM+10%FBS and were left overnight to settle. Then 0.1M HCl was used to make a media with pH 6. Next, this media was added to the cells and were left for 6 hours. Then the morphology of the cells was assessed under the bright field microscope. In low-pH conditions, the cells tend to minimize the surface-to-volume (S/V) ratios <sup>6</sup>. Our observations illustrated that size of the cells were decreased in pH 6.0 compared to pH 7.4 and the shape of the cells changed towards more round shape compared to flatten and triangle shape of the cardiac fibroblasts in pH 7.4. In pH 6, it was observed that some of the cells were white round-shape and were starting to detach from the surface due to the low protein attachment factors which results from cells going through the apoptosis phase. This suggests that low pH is not the optimum pH environment for the cell viability. However, majority of the cells in both conditions were attached to the surface and thus are alive. Therefore, these observations demonstrated that the morphology and the S/V ratios of cardiac fibroblasts were changed in response of the changing pH level of the environment.

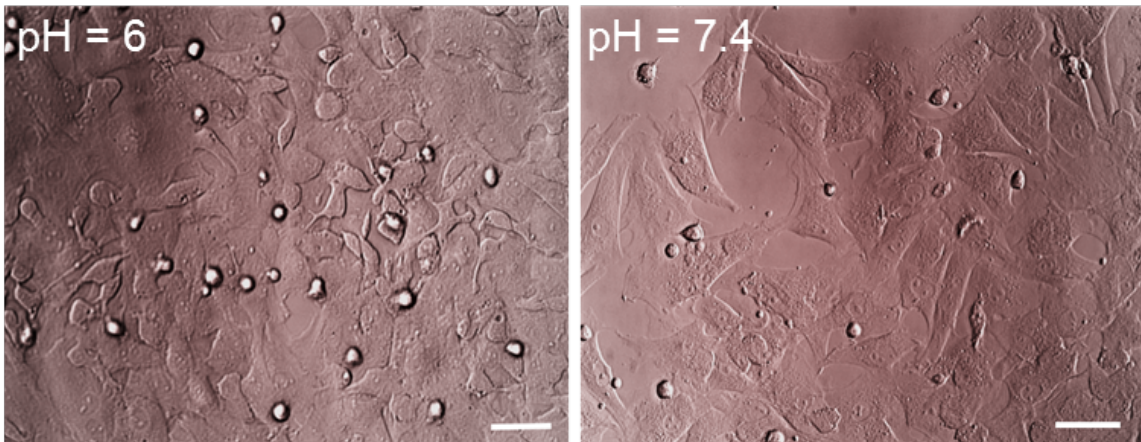


**Figure SI 10.** Cells morphology in pH=6.0 vs pH=7.4. Bright field images illustrated that cells size decreased in pH= 6.0 compared to pH= 7.4. Also, shapes of the cells were more round shape in pH= 6.0 compared to flatten and triangle shape in pH= 7.4. Scale bar 50 $\mu$ m.

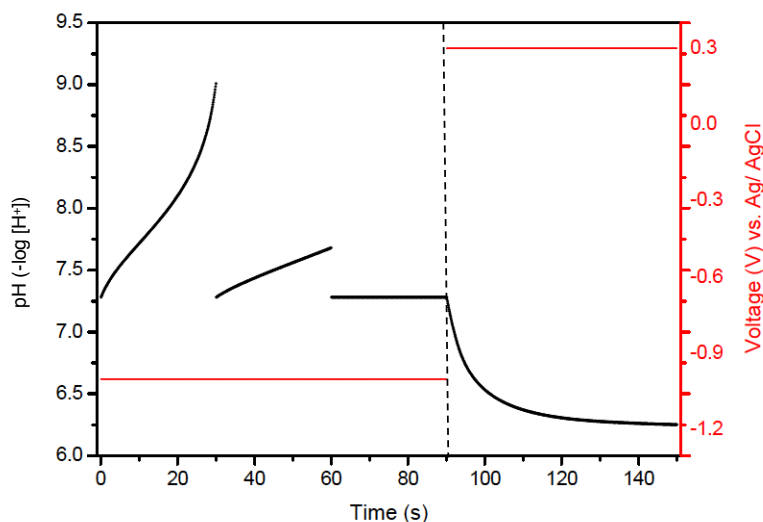


**Figure SI 11:** The bioelectronics triggering of MPs at the interface of cardio fibroblast. In this experiment we started with media pH= 7.4 while the fibroblast cells are already cultured on top of Pd NPs contacts. The pH changes from pH= 7.4 to pH= 9.0 upon application of V= -1.0V vs. RE for 30 sec. We replaced the solution with a fresh media pH=7.4. The pH changes from pH 7.4 to pH 7.7 upon application of V= -1.0V vs. RE for the second 30 sec. We again replaced the solution with a fresh media at pH 7.4. We did not see any significant change in the pH of the media solution upon application of V= - 1.0V vs. RE for the third 30 sec. We replaced the solution with the fresh media at pH 7.4

containing 500  $\mu\text{g/ml}$  MPs. Upon application of  $V = +0.3 \text{ V}$  vs. RE the pH changed from  $\text{pH} = 7.4$  to  $\text{pH} = 6.2$ . This pH change triggered the MPs and releases the FDA.

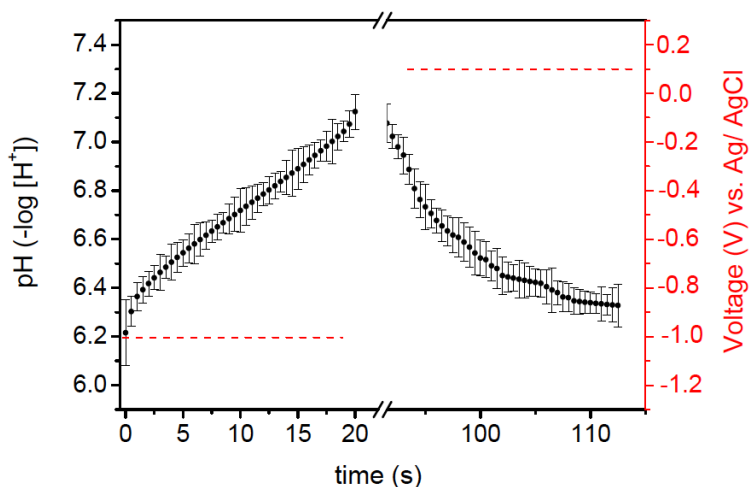


**Figure SI 12:** The bioelectronics triggering of MPs at the interface of cardio fibroblast. In this experiment we started with media  $\text{pH} = 6.2$  while the fibroblast cells are already cultured on top of Pd NPs contacts. The pH changes from  $\text{pH} 6.2$  to  $\text{pH} 7.1$  upon application of  $V = -1.0 \text{ V}$  vs. RE for 20 sec. We replaced the solution with the fresh media  $\text{pH} 7.4$  containing 500  $\mu\text{g/ml}$  MPs. Upon application of  $V = +0.1 \text{ V}$  vs. RE the pH changed from  $\text{pH} 7.4$  to  $\text{pH} 6.2$ . This pH change triggered the MPs and releases the FDA. We used the same PdH electrode for several experiment (the data are collected from 3 different experiment using the same PdH electrode). The calculated standard deviation is greater than 0.035 and less than 0.099 confirming the stability of PdH electrodes upon changing the pH in several experiments.

### Control experiment for FDA-released MPs using bioelectronic device

We applied a control experiment to find out whether FDA uptake within the cells was only due to the reduction of pH through the release of  $H^+$  flows within the solution and not as a result of the electroporation which created pores on the cell membrane upon the application of electric field<sup>7,8</sup>. In order to perform this experiment, cells were seeded on Pd NPs and media containing MPs (pH 6) were added to the cells. Then negative voltage  $V=-1V$  vs. Ag/AgCl was applied for 20 sec and this step was repeated for three times. However, the application of positive voltage as the second part of the process was excluded to prevent the H oxidation. Then, FDA uptaken were assessed under the fluorescent microscopy after 1hr. Microscopic observation did not show any FDA uptaken within the cells which confirmed that FDA is only released and uptaken within the cells in low environmental pH and not due to the electroporation.

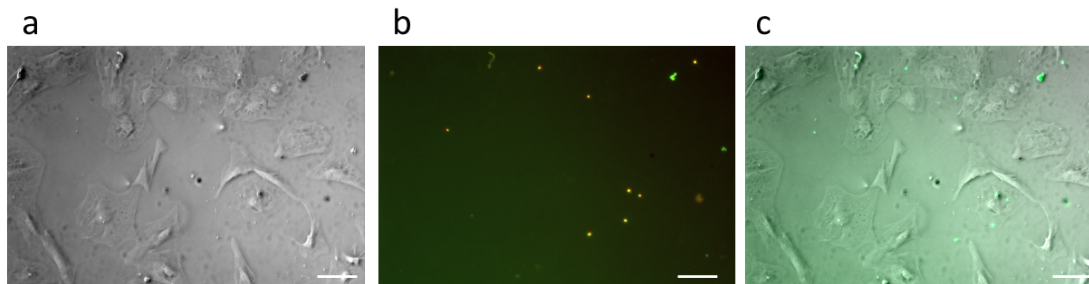


**Figure SI 13:** Electronic stimulation of cell membrane in presence of MPs on Pd NP device. Cardiac fibroblasts were plated on fibronectin coated Pd NPs. MPs were then added to the cells. Then cells were exposed to negative voltage ( $V=-1V$  vs. Ag/AgCl) 20 sec for three times. Fluorescence images of the cells captured 1hr after electrical stimulation. (a) Bright field image of the cells. (b) Rho-MPs + FITC image of the cells.

(c) Bright field + FITC image of the cells did not show fluorescein uptake into the cells.

Scale bar 100 $\mu$ m.

#### Assessment of cell number before and after electronic stimulation

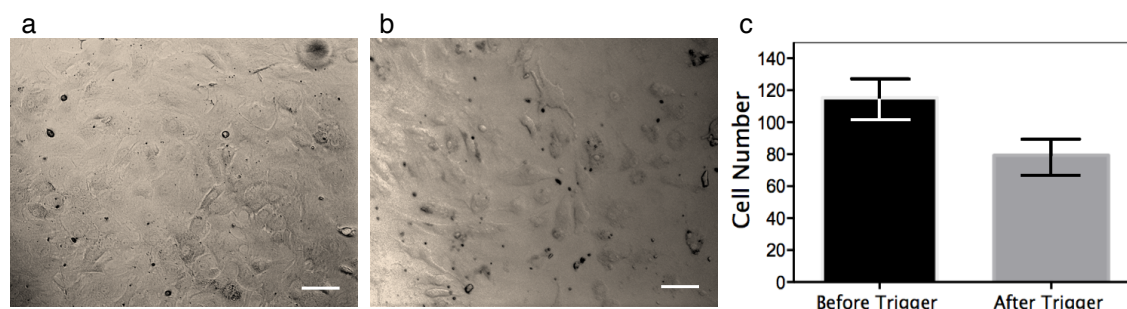


**Figure SI 14:** Phase contrast images (a) before (a) and (b) after three times repeated electronic stimulation; Cell were counted before and after electronic stimulation using ImageJ. (c) Statistical analysis illustrated that although cell number decreased after stimulation, however, this reduction was not significant. Scale bar is 100 $\mu$ m.

#### References

- (1) Dencher, N. A. H., J.; Bu" ldt, G.; Ho"ltje, H. D.; Ho"ltje, M., Membrane Proteins: Structures Interactions and Models Pullman,. Pullman,A.; et al., Eds., Kluwer Academic Publisher: 1992; p 69.: 1992.
- (2) Bachelder, E. M.; Beaudette, T. T.; Broaders, K. E.; Dashe, J.; Fréchet, J. M. Acetal-derivatized dextran: an acid-responsive biodegradable material for therapeutic applications. *Journal of the American Chemical Society* **2008**, *130* (32), 10494-10495.
- (3) Khademhosseini, A.; Eng, G.; Yeh, J.; Kucharczyk, P. A.; Langer, R.; Vunjak-Novakovic, G.; Radisic, M. Microfluidic patterning for fabrication of contractile cardiac organoids. *Biomed Microdevices* **2007**, *9* (2), 149-157, DOI: 10.1007/s10544-006-9013-7.
- (4) Zhu, K.; Shin, S. R.; Kempen, T. v.; Li, Y.-C.; Ponraj, V.; Nasajpour, A.; Mandla, S.; Hu, N.; Liu, X.; Leijten, J.; Lin, Y.-D.; Hussain, M. A.; Zhang, Y. S.; Tamayol, A.; Khademhosseini, A. Gold Nanocomposite Bioink for Printing 3D Cardiac Constructs. *Advanced Funcional Materials* **2017**, *27* (12).
- (5) Po, H. N.; Senozan, N. The Henderson-Hasselbalch equation: its history and limitations. *J. Chem. Educ* **2001**, *78* (11), 1499.

- (6) Černá, K.; Neustupa, J. The pH-related morphological variations of two acidophilic species of Desmidiaceae (Viridiplantae) isolated from a lowland peat bog, Czech Republic. *Aquatic ecology* **2010**, *44* (2), 409-419.
- (7) Saulis, G.; Saulė, R. Size of the pores created by an electric pulse: Microsecond vs millisecond pulses. *Biochimica et Biophysica Acta (BBA)-Biomembranes* **2012**, *1818* (12), 3032-3039.
- (8) Brownell, W. E.; Qian, F.; Anvari, B. Cell membrane tethers generate mechanical force in response to electrical stimulation. *Biophysical journal* **2010**, *99* (3), 845-852.